FWI Imaging: Revealing the unprecedented resolution of seismic data

Zhiyuan Wei*, Jiawei Mei, Zedong Wu, Zhigang Zhang, Rongxin Huang, Ping Wang (CGG)

Summary

Although the resolution of a seismic image is ultimately bound by the spatial and temporal sampling of the acquired seismic data, the seismic images obtained through conventional imaging methods normally fall far short of this limit. In addition to attenuation in the Earth, factors such as velocity errors, illumination holes, residual noise and multiples, source and receiver ghost notches, and migration swings can prevent conventional imaging methods from obtaining a high-resolution image of good signal-to-noise ratio (S/N) and well-focused details as promised by the maximum migration frequency. Recently, FWI Imaging, which uses the full-wavefield data to iteratively invert for the reflectivity together with velocity through full-waveform inversion (FWI), has shown to be a superior method for providing seismic images of greatly improved illumination, S/N, focusing, and thus better resolution, over conventional imaging methods. Here, we push FWI Imaging to a frequency close to the temporal resolution limit of seismic data (100 Hz) and demonstrate that FWI Imaging at a very high frequency can provide seismic images of unprecedented resolution from the recorded data, which has been impossible to achieve by other seismic imaging approaches.

Introduction

A high-resolution seismic image is of great importance to exploration and production in many ways, such as bypassing drilling hazards and identifying compartmentalized reservoirs. The resolution of a seismic image is determined by its effective bandwidth within which reasonable S/N is present. Therefore, seismic resolution is mostly dictated by three parts: 1) the low-wavenumber resolution that is primarily determined by the lowest frequency component in the recorded data; 2) the high-wavenumber vertical and lateral resolution that is determined by the highest frequency component in the recorded data, as well as the spatial sampling of sources and receivers; and 3) an accurate velocity model with proper low- and high-wavenumbers to correctly map the full-bandwidth seismic data in the time domain to an image in the depth domain. In addition, illumination holes, residual noise and multiples, and migration artifacts can introduce noise to the migration image and degrade the S/N and resolution.

The conventional seismic imaging process takes more of a linear approach to this problem, with numerous steps designed in preprocessing, velocity model building (VMB), migration, and post-processing to solve one or a few specific issues at each step. For instance, to improve the low-

frequency content in the data, deghosting that removes the source- and receiver-side ghosts can be performed to increase the low-frequency S/N of the input data, and thus improve the low-wavenumber resolution of migration images (Wang et al., 2013). However, the efficacy of deghosting is often limited by the spatial sampling and S/N of the input data. Another case in point is multiple attenuation, which is not only time consuming but it is also very difficult to completely remove multiples without damaging primary signals. More importantly, valuable information contained in the multiple energy that is essential for both vertical and lateral resolution is discarded. Migration of multiples (Yang et al., 2013) has been proposed to use the reflection multiples as input to infill illumination holes of primary energy and improve the vertical and lateral resolutions over primary migrations. However, migration of multiples generally suffers from crosstalk noise among primaries and different orders of multiples (Yang et al., 2015). Although least-squares migration of multiples (Wong et al., 2014) can mitigate the crosstalk noise to some extent through an iterative least-squares data-fitting process, such approaches often still require primary-multiple separation because the modeling engine can only simulate part of the energy in the recorded full-wavefield data. In addition, they need to use a velocity model obtained by separate VMB approaches with different input data and objective functions, which is usually not optimal to collapse all the multiple energy used in the least-squares migration of multiples. In short, the limits of individual steps and the disconnects between them make it difficult for conventional imaging processes to deliver a high-resolution image with well-focused details as implied by the maximum migration frequency.

Maximizing seismic resolution with FWI Imaging

FWI Imaging (Zhang et al., 2020), which models and uses the full-wavefield data, including primaries and multiples (ghost included) and reflection and transmission waves, to iteratively invert for the reflectivity together with velocity, is a systematic approach to the seismic imaging problem and provides an elegant solution to mitigate most of the previously discussed limits imposed on conventional imaging approaches. Next, we will explain how FWI Imaging can extract the full benefit of seismic data for optimal low- and high-wavenumber resolution with superior S/N and focusing.

Noise attenuation is a necessary step in conventional imaging approaches to improve the S/N of migration input data. However, noise attenuation at the low-frequency end is difficult because the S/N is often very low and denoise is

only performed in local windows dealing with small subsets of the wavefield separately. For these reasons, the output from those approaches often still contains considerable residual low-frequency noise with compromised low-frequency signals. FWI Imaging, on the contrary, can use input data with minimal preprocessing so that low-frequency signals are properly retained. In addition, FWI Imaging works on the entire wavefield recorded by all the shots and receivers in a survey and can utilize low-wavenumber information contained in large-angle data (e.g., diving waves) that cannot be used in conventional imaging approaches. Moreover, by running the inversion with many iterations at each frequency step, FWI Imaging can extract the low-wavenumber information as much as possible from the low-frequency data. Lastly, FWI Imaging can accurately handle low-frequency ghost effects by directly simulating them in the modeling engine and hence can further improve the low-wavenumber resolution.

As for higher wavenumbers, there are two factors that enable FWI Imaging to provide increased vertical and lateral resolution. First, FWI models different orders of multiple energy, which offers additional small-angle near-vertical illumination on top of primary energy and increases both vertical and lateral resolution of images. Second, diving wave energy, which is treated as noise in conventional imaging methods, can be properly utilized in FWI Imaging. As the diving wave energy travels horizontally with large angles, it can better resolve the lateral velocity variations and subsequently improve the lateral resolution of images.

Finally, FWI Imaging obtains velocity and reflectivity in the same inversion, and therefore, the velocity is automatically consistent with the image for optimal focusing of all the energy. By iteratively updating velocity from low to high frequencies, FWI Imaging provides a proper low- and high-wavenumber velocity that can focus the full-bandwidth seismic data. With iterative least-squares fitting of the full-wavefield data, migration artifacts, noise in the input data, and illumination issues due to imperfect acquisitions, which often manifest in conventional migration images, are automatically minimized in FWI Images (Huang et al., 2021).

We performed FWI Imaging at 100 Hz on a streamer field data set to demonstrate how FWI Imaging is able to effectively reveal subsurface geological details with an unprecedented resolution that is impossible to achieve by other seismic imaging approaches.

Source-over-spread streamer data in the Barents Sea

To assess FWI Imaging's benefits, we examine its results on a streamer data set and compare it to conventional Kirchhoff, which is commonly considered to be the go-to product for high-resolution images. The data set comes from a source-over-spread narrow-azimuth towed-streamer survey (NATS) in the Greater Castberg area of the Barents Sea. This area features an iceberg-scoured, highly rugose water bottom with shallow gas anomalies, which poses challenges for imaging the faulty area in the deeper section.

In this survey, a group of 5 sources with a horizontal span of 300 m and firing every 37.5 m along the inline direction are placed at the center of 16 slant-towed streamers to acquire the near offsets for shallow imaging. Another front source is
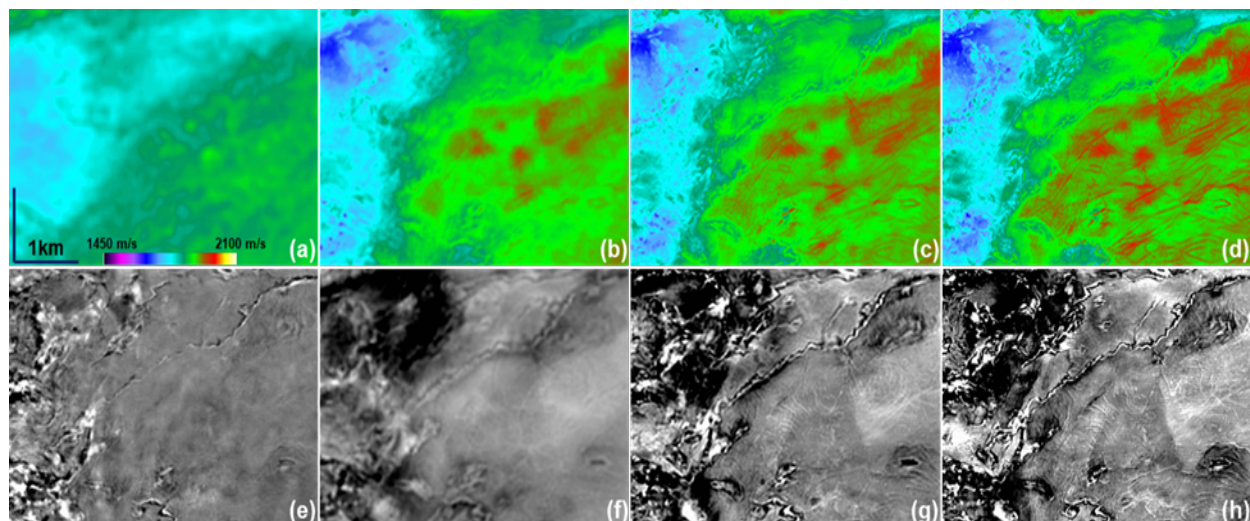

Figure 1: Depth slices at 600 m of a source-over-spread NATS data set in the Barents Sea. (a) 15 Hz TLFWI model, (b) 25 Hz TLFWI model, (c) 50 Hz TLFWI model, (d) 100 Hz TLFWI model. (e) 100 Hz Kirchhoff image with the 15 Hz TLFWI model in (a), and (f) – (h) are the FWI Images from the TLFWI models in (b) – (d), respectively. High-frequency FWI Images show improved structural details such as faults and channels.
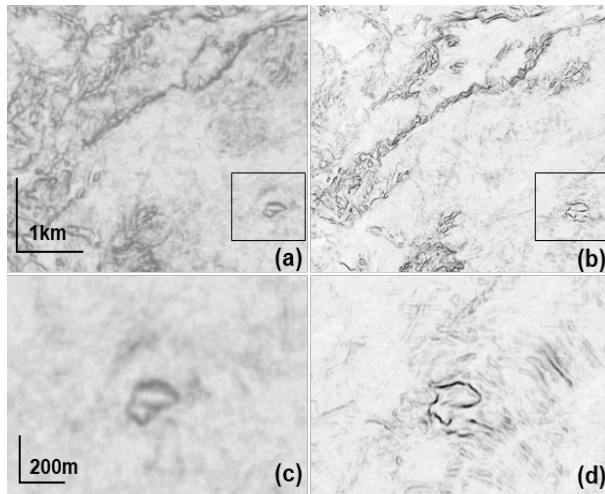
Figure 2: Depth view at 600 m of the coherence attribute extracted from (a) 100 Hz Kirchhoff image with the 15 Hz TLFWI model as shown in Figure 1a, and (b) 100 Hz FWI Image as shown in Figure 1h. (c) and (d) are the zoomed-in displays of the areas marked by the black rectangles in (a) and (b), respectively. High-frequency FWI Imaging provides superior resolution over Kirchhoff images.

towed by the streamer vessel to provide long offsets up to 8.2 km for VMB (Vinje et al., 2017). The cable spacing is 60 m between streamers, and the receiver interval within each cable is 12.5 m.

With the acquired data right after deblending without any further processing, we ran Time-lag FWI (TLFWI) (Zhang et al., 2018) from the lowest usable frequency of the data at 3 Hz up to the imaging frequency at 100 Hz and compared the FWI Images with the Kirchhoff results. Figures 1a-1d show depth slices at 600 m of the TLFWI models from 15 Hz, 25 Hz, 50 Hz, and up to 100 Hz, which gradually reveal more details in the velocity models as the frequency increases. Correspondingly, the resolution of the FWI Images continues improving when moving to higher frequencies, as shown in Figures 1f-1h. Figure 1e is the Kirchhoff image with the 15 Hz TLFWI model using the input data that went through a conventional processing flow, including denoise, deghost, and demultiple. As we can see, the image quality of the 100 Hz FWI Image is much better than the 100 Hz Kirchhoff image, with more clearly defined fault planes and better imaged small channels and other geological details. These features are either less obvious or completely missing in the counterpart Kirchhoff image. We can also observe better imaged geological details from the coherence attribute extracted from the seismic images (Chopra and Marfurt, 2017). The coherence attribute from the FWI Image (Figures 2b and 2d) shows more clearly defined small-scale features of better S/N than that from Kirchhoff (Figures 2a and 2c).

The improved vertical and lateral resolution of the FWI Images can also be observed from the section views, as shown in Figure 3. Similar to the observations in the depth slices, the resolution of the FWI Images from 25 Hz, 50 Hz,
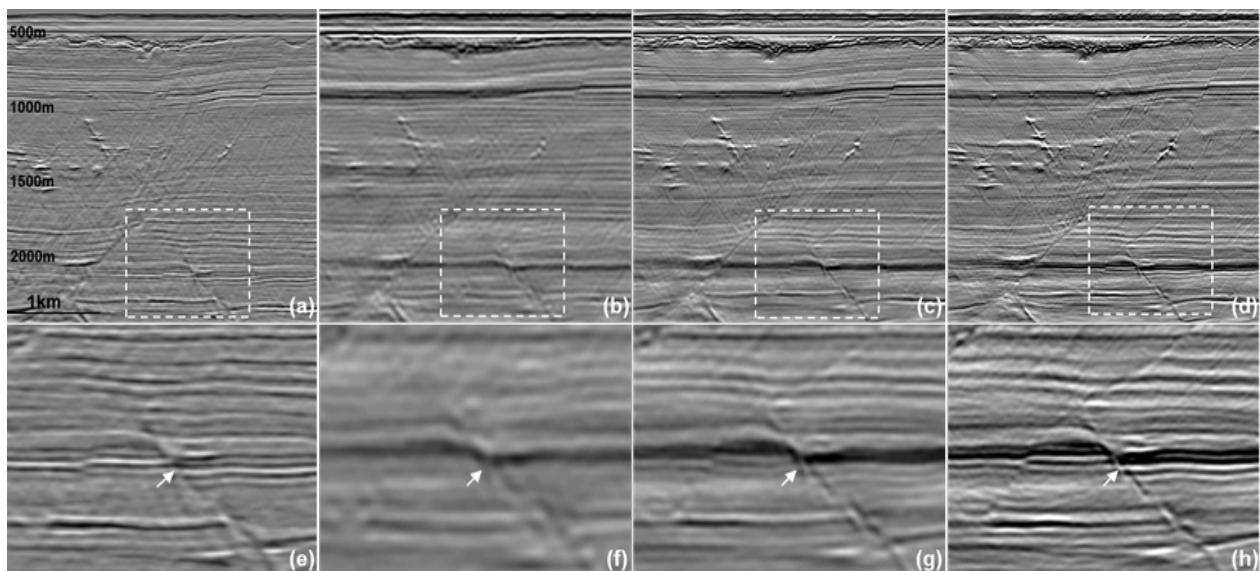

Figure 3: Section view of a source-over-spread NATS data set in the Barents Sea. (a) 100 Hz Kirchhoff image with the 15 Hz TLFWI model, (b) 25 Hz FWI Image, (c) 50 Hz FWI Image, (d) 100 Hz FWI Image. (e) – (h) are the zoomed-in displays of the white dashed rectangles in (a) – (d), respectively. High-frequency FWI Imaging provides well-focused geological details, such as faults.
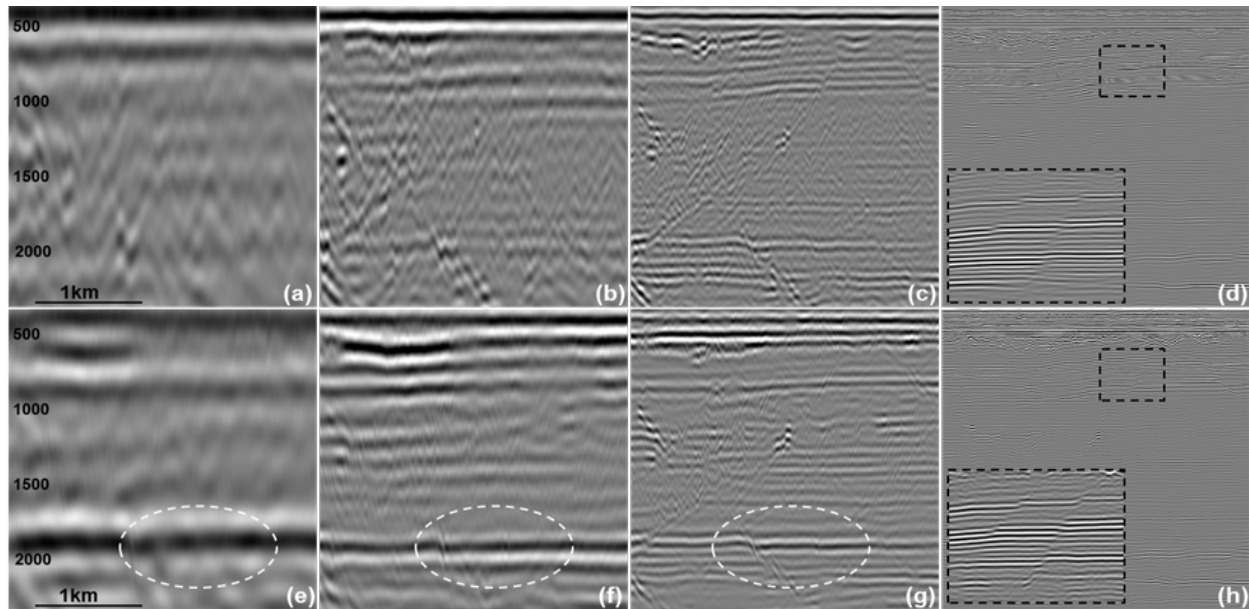
Figure 4. Section view of band-limited stack images from a source-over-spread NATS data set in the Barents Sea. (a) 0-4 Hz Kirchhoff stack, (b) 4-8 Hz Kirchhoff stack, (c) 8-16 Hz Kirchhoff stack, (d) 64-100 Hz Kirchhoff stack, (e) 0-4 Hz FWI Image, (f) 4-8 Hz FWI Image, (g) 8-16 Hz FWI Image, and (f) 64-100 Hz FWI Image. Better S/N is observed in the FWI Images at low, mid, and high frequencies.

and up to 100 Hz progressively improves. Structures such as faults are more precisely defined in higher frequency FWI Images, and the 100 Hz FWI Image overall shows a much better resolution than the 100 Hz Kirchhoff image. It is also worth noting that the FWI Images have a broader bandwidth than the Kirchhoff images based on the band-limited images shown in Figure 4. From the images in different frequency bands, 0-4 Hz, 4-8 Hz, 8-16 Hz, and 64-100 Hz, we notice that the S/N of FWI Images are overall better than the Kirchhoff images. Particularly, the FWI Image at the very low-frequency end (Figure 4e) shows coherent events that consistently appear in higher frequency images (Figures 4f-4g), while such events are missing in the Kirchhoff image (Figure 4a). This indicates that FWI can better compensate for the ghost effect through modeling and thus improve the low-frequency S/N. At the high-frequency end, the fault energy is better focused in the FWI Image (Figure 4h), while the Kirchhoff image (Figure 4d) suffers from contamination of migration swings that overshadow the subtle faults.

Discussion and conclusions

We demonstrated that FWI Imaging is able to extract the full benefits of seismic data and yields unprecedented image resolution that has been impossible to achieve with other imaging approaches. FWI Imaging can elegantly resolve issues such as velocity errors, migration artifacts, residual noise and multiples, and ghost effects in one (iterative) inversion. Additionally, proper handling of diving waves

and multiple energy in the FWI improves the vertical and horizontal resolution of images.

Spatial aliasing is typically not the bottleneck for low-frequency FWI for VMB (Mei et al., 2019), but it could be an issue for high-frequency FWI Imaging. Additional illumination from diving waves and multiple energy have made FWI Imaging less sensitive to spatial aliasing issues than conventional imaging methods. However, if the spatial sampling of the input data is too sparse, the acquisition footprint could manifest in the high-frequency FWI Images. This suggests that acquiring denser data is still important for high-resolution FWI Images.

It is worth noting that crosstalk noise and artifacts can still be observed in the high-frequency FWI Images if the input data is insufficient to ensure a good convergence of the velocity model at the low-frequency end (e.g., <10 Hz) and if there is inadequate physics in the FWI modeling engine and inversion algorithm, e.g., density, absorption, anisotropy, and elasticity may not be modeled or allowed to change during FWI. This presents room for future improvements of FWI Imaging from both the acquisition and algorithm sides.

REFERENCES

Chopra, S., and K. J. Marfurt, 2017, Coherence attribute applications on seismic data in various guises: 87th Annual International Meeting, SEG, Expanded Abstracts, 3416–3421, doi: https://doi.org/10.15530/urtec-2018 2886034.

Huang, R., Z. Zhang, Z. Wu, Z. Wei, J. Mei, and P. Wang, 2021, Full-waveform inversion for full-wavefield imaging: Decades in the making: The Leading Edge, **40**, 324–334, doi: https://doi.org/https://doi.org/10.1190/tle40050324.1.

Mei, J., Z. Zhang, F. Lin, R. Huang, P. Wang, and C. Mifflin, 2019, Sparse nodes for velocity: Learnings from Atlantis OBN full-waveform inversion test: 89th Annual International Meeting, SEG, Expanded Abstracts, 167–171, doi: https://doi.org/10.1190/segam2019-3215208.1.

Vinje, V., J. E. Lie, V. Danielsen, P. E. Dhelie, R. Silliqi, C.-I. Nilsen, E. Hicks, and A. Camerer, 2017, Shooting over the seismic spread: First Break, **35**, 97–104, doi: https://doi.org/10.3997/1365-2397.35.6.89461.

Wang, P., S. Ray, C. Peng, Y. Li, and G. Poole, 2013, Premigration deghosting for marine streamer data using a bootstrap approach in tau-p domain: 83rd Annual International Meeting, SEG, Expanded Abstracts, 4221–4225, doi: https://doi.org/10.1190/segam2013-0225.1.

Wong, M., B. Biondi, and S. Ronen, 2014, Imaging with multiples using least-squares reverse time migration: The Leading Edge, **33**, 970–976, doi: https://doi.org/10.1190/tle33090970.1.

Yang, Z., L. Chernis, W. Gou, S. Ji, Y. Li, and J. Hembd, 2013, Enhanced reverse time multiple migration and its applications: 83rd Annual International Meeting, SEG, Expanded Abstracts, 4121–4125, doi: https://doi.org/10.1190/segam2013-0776.1.

Yang, Z., J. Hembd, H. Chen, and J. Yang, 2015, Reverse time migration of multiples: Applications and challenges: The Leading Edge, **34**, 780–786, doi: https://doi.org/10.1190/tle34070780.1.

Zhang, Z., J. Mei, F. Lin, R. Huang, and P. Wang, 2018, Correcting for salt misinterpretation with full-waveform inversion: 88th Annual International Meeting, SEG, Expanded Abstracts, 1143–1147, doi: https://doi.org/10.1190/segam2018-2997711.1.

Zhang, Z., Z. Wu, Z. Wei, J. Mei, R. Huang, and P. Wang, 2020, FWI imaging: Full-wavefield imaging through full-waveform inversion: 90th Annual International Meeting, SEG, Expanded Abstracts, 656–660, doi: https://doi.org/10.1190/segam2020-3427858.1.